InstruQuest, Inc.
December, 2021

Bubble Point and Capillary Flow Porometer

By Jan Malczyk

Better implementation of the Bubble Point and Capillary Flow Porometer (CFP) techniques are presented as optional capabilities that can be implemented in the pV/T Master volumetric analyzer. Improved theoretical approach and critical remarks that are often omitted in commercial marketing of such products are also presented.

In the Capillary Flow Porometer technique, the so called “dry run” should be normally carried out first as wetted and dried samples may not have the same properties as the unmodified dry samples. Typically a series of increasing flow rate steps is applied under the dry sample mounted in a sample holder. The corresponding pressure values resulting from the specimen flow resistance are recorded. The next stage is to run the same experiment but with the wetted specimen, the so called “wet run”. Usually, the first task of the wet run is determination of the largest pore size using the bubble point method. Depending on the design of a particular experimental setup, either the pressure values are set as the independent variable and the resulting gas flow rates are the response, or the known flow rates are set as the independent variable and the resulting pressure values are the response. Traditionally, the flow rates (ordinate) are plotted versus pressure data (abscissa) of both runs, and information about the pores of the specimen is extracted.

This simple concept of the Bubble Point and Capillary Flow Porometer techniques is the only simple thing about this approach. There are many technical problems in practical implementation of the techniques and interpretation of the results seems to be questionable. The high flow rates used in these instruments do not seem to be of much of value other then testing the flow resistance at high flow rates for some limited applications. But it is the pore size distribution function as the essence of this technique that needs to be revisited.

The Density Functional Theory, initially devised for quantum mechanics applications, was adopted for modeling pore size distribution in porous materials using physical adsorption isotherms. Except being a mathematical exercise, the whole approach seems to be of little if any practical value. But considering popularity of such approach at that time, it is no surprising that its formulation for capillary flow porometry took the following form:

$$\frac{F_W}{F_D} = \int_{Rmin}^{Rmax} f(r)\,dr \qquad \text{Eq. 1}$$

where F_W and F_D are the wet and dry flow rates, f(r) is the pore size distribution function, Rmin and Rmax are the minimum and maximum pore sizes.

Calculating derivative of the equation with respect to r and from the definition of the quotient derivative, the more practical version is commonly used for processing of experimental data:

$$\frac{\left(\frac{F_{W(j+1)}}{F_{D(j+1)}} - \frac{F_{W(j)}}{F_{D(j)}}\right)}{\Delta r} = f(r) \qquad \text{Eq. 2.}$$

where $F_{W(j+1)}$ and $F_{D(j+1)}$ are the wet and dry flows in the experimental step j+1, $F_{W(j)}$ and $F_{D(j)}$ are the wet and dry flows in the previous step j, and the Δr is absolute difference between the pore sizes r_j -r_{j+1} corresponding to the pressure interval in the j and j+1 steps.

While it is expected that additional pores will be opened when increasing pressure step from P_{Wj} to $P_{W(j+1)}$, it is by no means guaranteed. Claiming that the flow through pores of radius between r_j and r_{j+1} is equal to $\left(\frac{F_{W(j+1)}}{F_{D(j+1)}} - \frac{F_{W(j)}}{F_{D(j)}}\right)$ does not seems to be convincing. Flow at the next pressure step P_{j+1} is the sum of flows through existing (already opened pores) at this higher pressure and the additionally opened pores (if any) due to the pressure step increase from P_j to P_{j+1}. It is difficult to say, what is the contribution to the flow from only the newly opened pores, unless the flow through already opened pores can be approximated by a known relationship of flow versus pressure. Therefore, the frequently repeated interpretation and calculations used for the pore size distribution in the CFP implementations do not seem to be correct.

Considering the vast variety of porous materials and their complex structure, it is difficult to propose a universal relationship between the flow and pressure steps for the dry flow. Some thin samples like etched or laser drilled films may require approach similar to modeling of flow through orifices. Due to rather well defined shapes and sizes, optical methods are perhaps more suitable for their pores determination then the use of CFP. Samples with large size pores that can barely hold the wetting liquid may not be easily measured by the CFP and perhaps a profile close to linear relationship can be used. **But samples containing relatively small pores can be approximated by the equation of gas flow through capillaries taking into account comprehensibility of gas and this approach and usage of much lower flow rates along with different interpretation of results is being proposed for the CFP technique.**

The CFP technique can be easily implemented in the pV/T Master volumetric analyzer as an optional capability that can be added at any time. This can be achieved at a fraction of the cost of a separate, bulky, and expensive instrument. From the filtration point of view, only the largest pores are relevant so there is no need for extensive flow and pressure ranges. Usage of one mass flow controller (MFC) is sufficient as different apertures can be used to achieve higher flow rates per unit of area. Although the CFP option can be implemented by adding the suitable hardware directly over the sample chamber, it is far more convenient to have an external fixture interfaced with the main instrument. The picture of the pV/T Master and the external station is presented below.

One of the main design objectives was to allow the user visually observe the process, especially the bubble point onset. The relatively large borosilicate glass tube has a detachable flash light mounted at the top of the upper adapter. Second port of the adapter allows for introduction of liquid and its removal using a large capacity syringe with flexible tubing. The gas supply port and connection to pressure transducer are located at the base. Input to the manual valve is also connected to the base and its output is connected to the back-pressure regulator. Modular design of the sample mounting assembly allows the sample manipulation to be done outside of the station and install the assembly into the station for

tightening. Auxiliary side port can be used for evaluating of longitudinal flow in addition to the perpendicular flow of gas through the sample. Depending on particular design of adapters, either the sample needs to be of circular shape of up to 63 mm (about 2.5”) in diameter to fit into the assembly or no cutting is required as practically any flat piece that can be fitted into the station can be measured.

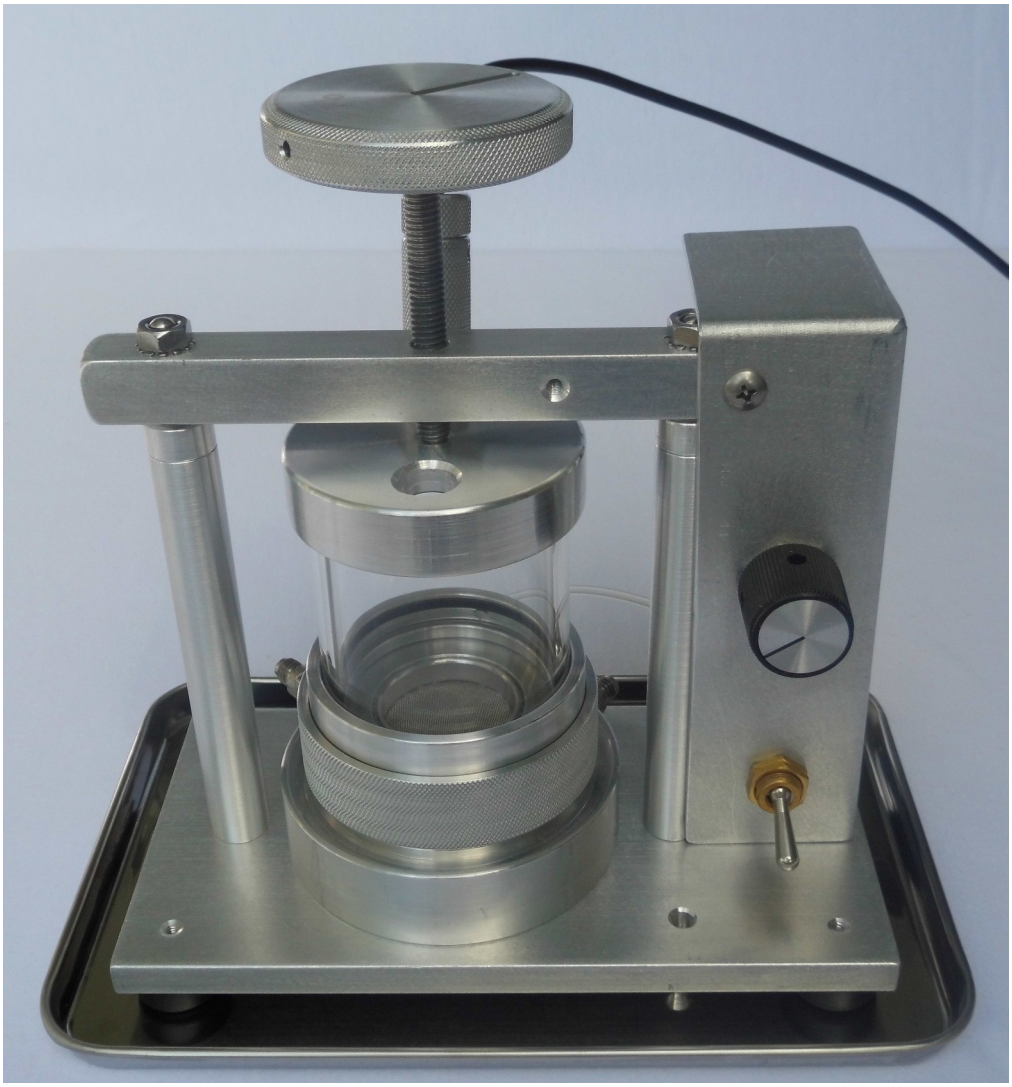

Bubble Point and Capillary Flow Porometer station (Fig. 1)

The design of the sample mounting and its support, from the top and bottom of it, is very important as it can affect the overall results, especially for “wet” runs. Different approaches and trade offs need to be evaluated for different types of samples as there is no ideal way of somehow holding the sample in plane without affecting its integrity and hoping only for the passage of gas through the designated area. In the “dry” runs, when pressure or flow is increased, many samples exhibit increased lateral flow and the overall effect is as if the effective sample area restricted by O-ring or rubber disc is increasing. The amount of force pressing the sample in its housing is user controlled by using the large knob.

The automatic and manual operations are available for the user to evaluate usefulness of the technique for particular research objectives. Using the auxiliary experiment definition template, the user can

declare any set of flow rates within the mass flow controller (MFC) range, declare pause (until the wetting of the sample and bubble point is determined after the dry run), and declare repeating the same set of flow rates for the wet run. As an example, the results of the five times repetitions of the dry run are presented below.

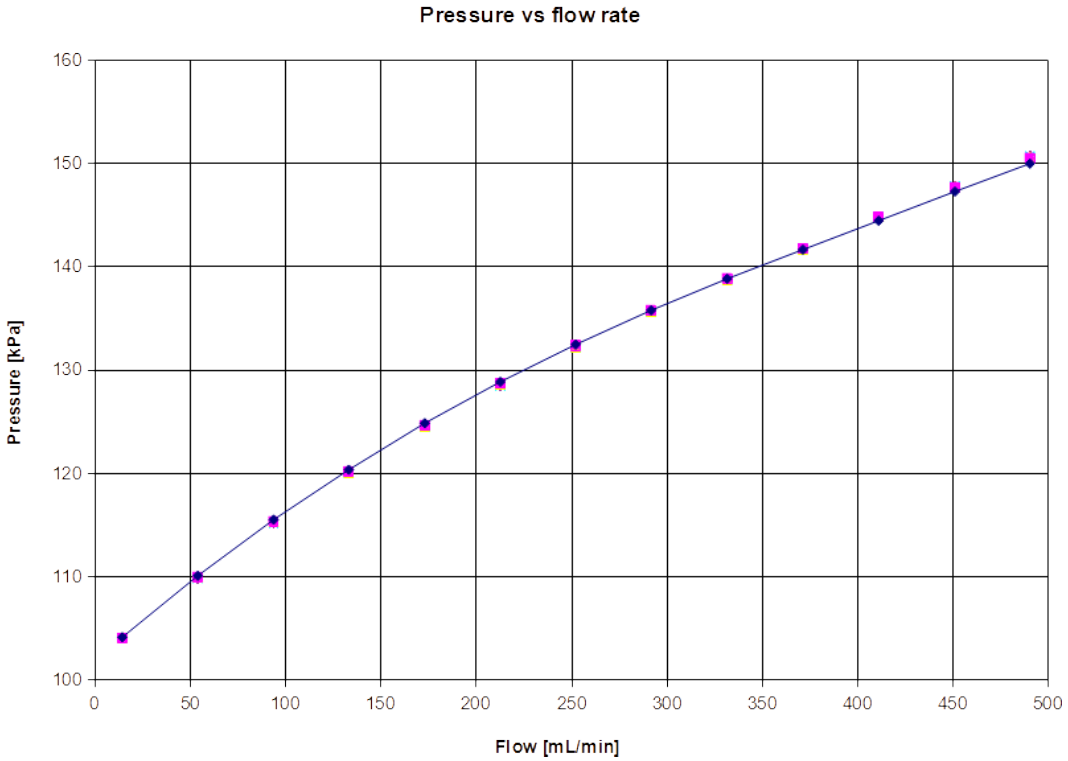

Dry run, five repetitions (Fig. 2)

The dry runs are fairly repeatable and show non-linear relationship of flow versus pressure data, opposite to linear profiles presented in many presentations of CFP principles. If the specimen sample contains narrow passages which can be considered as capillaries, then the flow $\mathbf{f_c}$ through a single capillary is described by Poisseuille equation and its corrected version for compressible fluids (gases) can be used.

$$f_c = \frac{\pi \cdot R^4}{16 \cdot \mu \cdot h \cdot P_a} \cdot \left(P^2 - P_a{}^2\right) \qquad \text{(Eq. 3)}$$

where R is the radius of such equivalent capillary, $\boldsymbol{\mu}$ is the dynamic viscosity, **h** is the length of the capillary and it is often approximated as the thickness of the specimen (shortest capillary), **P** is the pressure at the input, $\mathbf{P_a}$ is pressure at the output, typically atmospheric pressure. Since the total dry flow $\mathbf{F_d}$ is the result of flows through many capillaries of different radii, the above equation can be rewritten is a more general form:

$$\text{Total dry flow } F_d = \frac{\pi \cdot \left(P^2 - P_a^2\right)}{16 \cdot \mu \cdot h \cdot P_a} \cdot A \cdot \sum_{i=1}^{N} n_i \cdot R_i^4 \qquad \text{(Eq. 4)}$$

Where A is the sample area, **N** is the total number of all capillaries, $\mathbf{n_i}$ is the number of capillaries of certain radius $\mathbf{R_i}$ per unit of area. From the equation form, it is conclusive that rather a quadratic

relationship is expected between the flows and pressures values. Departures from the quadratic dependence can be related to several situations, like:

1. The sizes of the passages are relatively large and rather linear relationship is observed in the flow range used.
2. Incorrect mounting of specimen causing crushed sample at the place of mounting.
3. Holes in the specimen or ruptured or stretched specimen under the used flow/pressure conditions,
4. Incorrect implementation of the technique by measuring only the differential pressure across the specimen or just one pressure under the specimen while the output pressure is not at the assumed atmospheric pressure as it is the case in some closed-loop implementations when using high flow rates.

The proper implementation of the CFP requires either knowledge of input pressure (under the sample) and output pressure (over the sample) values, or at least the input pressure while the output pressure is sufficiently opened to the atmosphere to maintain the same atmospheric pressure value at all flow rates.

It is worth mentioning, that a simpler form of the equation 3 is used for incompressible fluids, like water, where the flow is directly proportional to the pressure drop (Darcy Law). Somehow, there are quite a large number of publications where for compressible fluids, like gases, such simpler form is used. So it is no surprising, that when working with gases and carrying out more accurate data processing, additional corrections are used to account for non-linear profiles. Thus, the validity of such results interpretations and the need for introduction of corrections can be disputed.

After finishing the dry run, the specimen needs to be wetted and reinstalled for the wet run. The first part of the wet run is finding the bubble point pressure. The determination of the pressure value at which first bubbles are emitted from a wetted sample under gas pressure is of importance in characterization of material designed for filtration as it yields the largest pore size. Seemingly a simple idea is not all that easy once the practical implementation is undertaken. There quite a few aspects to take care of and automation of such bubble point determination is rather not reliable.

Considering the variety of mechanical properties of porous membranes and interactions with various wetting agents, the proper design of sample chamber and the way of fastening of the sample plays a critical role in determining the correct onset of bubble(s) emission. The most common problem is that when the sample is squeezed between two metal surfaces, the bubble emission starts at the edges of metal contact and bubbles will appear at much lower pressures then the actual bubble point pressure. In many cases it is very difficult to achieve proper mounting due to the sample nature. Moreover, any further results obtained from the wet run will be also incorrect when bubbles start from the edges. In most commercially available CFP instruments the sample is installed inside a metal enclosure and there is no way to see what is happening there. Many samples require a mechanical support as they can get easily stretched by a pressure differential. The particular design of such support also plays a role in affecting contact spots with the sample and producing early onset of bubbles.

Th automatic determination of the bubble point is also problematic. Even if a low flow rate is used, like 10 to 50 mL/min depending on the ability of particular range of mass flow controller used, the determination of the bubble point pressure from the inflection point of initial diffusional rise in flow to where a sharp flow increase is noticeable, the actual breakthrough pressure can occur earlier then the one determined from the derivative of such pressure profile. Since the dead volume is often low and

fixed in CFP designs, the rate of pressure increase is relatively high which tends to increase the bubble point pressure. The marketing points of speed are at the expense of quality of results, and generally in many CFP instruments the results of bubble point determination are mostly inaccurate.

The ability to visually observe the emission of bubbles while increasing the pressure is a more reliable method then an automated one. As presented on the Fig. 2, the sample cell is extended by using pressure rated thick borosilicate glass tube and it can be illuminated by any suitable light source to facilitate visual observations of events while changing the pressure under the sample. The press-down force on the circular specimen is regulated by the top screw with round knob and the pressure is equally distributed, unlike in many threaded sample cell closure designs. The cell can be designed to hold samples of different thicknesses. The sample support and either flat rubber discs or O-rings can be be selected as suitable for a given filter material, depending on particular sample cell construction. Using the movable O-ring on cell perimeter (self centering design) prevents escape of gas through lateral flow path and is convenient for assembly and disassembly of the setup.

Once the wetted specimen has been installed and the whole assembly fastened to the main sample chamber of the station, additional amount of wetting liquid to reach few mm height can be added for easier observation of the bubbles. The best strategy of carrying out the visual observation of the emissions of bubbles is by using the Manual mode of operation and auxiliary back pressure regulator. Before any flow is applied, the valve knob should lifted up to allow flow into the back-pressure regulator which should be fully opened by turning the knob to the most counterclockwise position.

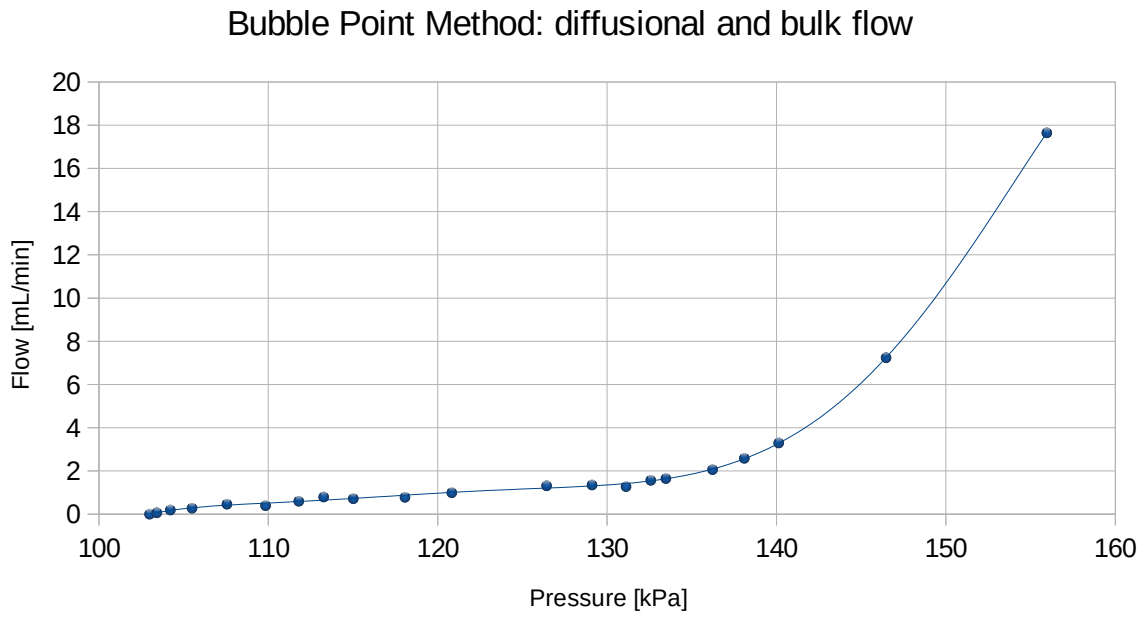

Visual observation of the onset of bubbles emission. (Fig. 3)

The flow provided by the mass flow controller (MFC) should be set to just above the minimum value specified by a given model. By slow adjustment of the back-pressure regulator knob, various pressure levels can be obtained. Initially, most of the flow is discarded by the flow path through the back-pressure regulator where it can be measured manually using a bubble flow meter to obtain the

diffusional flow values by calculating the difference between the MFC flow and the bubble flow meter flow. This approach can be advantageous to determine diffusional flow through large filters where it could be technically challenging to measure such flow directly from above the sample chamber. The ability to adjust the flow rate and consequently pressure to practically any value is advantageous for measurements of wide variety of samples. The amount of diffusional flow can be significant and it can far exceed the flow through the first open pore(s). The dead volume under the specimen can be controlled by using various reducing adapter(s) in the sample chamber or increased as needed by addition of the reference chamber volume.

The bubble point pressure may not be so easy to determine as initially the diffusional flow vs pressure can cause random formation of small bubbles on the specimen surface at various spots. Only when bubbles began to appear at the same spot in a repeatable way, and the location is not at the place of mounting, then this pressure can be considered as the bubble point pressure. When the pressure is increased, more bubbles appear at different places and more intense flow from the initial bubble spot(s) can be observed. By reducing the pressure to no visible flow conditions and trying to increase slowly the pressure again, the bubble point pressure may not necessarily be the same as the one initially determined but generally lower and clustered around the lower values in repeated attempts. The spread of values can be quite large, and can range from 137 to 131 kPa for the sample investigated.

The explanation of this behavior can be attributed to several aspects. Once the liquid from the bottom of the passage is pushed up then it might not get replenished to the same state as it was originally and the surface tension around this opening may change. More likely though, the high enough pressure to produce a stream of bubbles from the same spot affects the structure of the sample material, so it will be easier to get through the next time. The interaction of the wetting liquid with the specimen and the complexity of specimen structure needs to be considered. Also, the drying of the bottom of the wetted specimen over time can affect the minimum pressure needed to emit bubbles. The time of approach to the bubble point pressure is also a factor. Selection of suitable wetting agent for a given specimen and experimental conditions need to be carefully evaluated to arrive at repeatable results of bubble point pressure determination. The process of wetting of the sample can play a role. Carrying out the wetting at vacuum condition of thick samples would ensure liquid intake into small pores, which might not happen readily if the wetting is done at atmospheric pressure conditions.

Upon determination of the bubble point pressure, the more desirable practical information is how this pressure can be related to the size of the passage. It should be clearly understood that due to lack of a more meaningful approach and for simplicity reasons, only a crude approximation of passage size by assuming an equivalent circular opening (pore) is often used as presented in the formula below.

$$d = \frac{4 \cdot \sigma \cdot \cos(\Theta)}{\Delta P - \varsigma \cdot g \cdot h} \cdot 10^6 \qquad \text{Eq. 5}$$

where:

d – equivalent (ideal) pore diameter [μm]
σ – surface tension [N/m]
Θ – solid-liquid contact angle [degrees]
ΔP – pressure difference between the first bubble(s) emission and atmospheric pressure P_a [Pa]
ς – density of liquid [kg/m^3]
g – gravity of Earth [m/s^2]
h – height of the liquid above the sample [m]

The contact angle Θ is often assumed to be 0 and that results in the largest pore size as the cos(0) = 1. On the other hand, since the passing gas does not remove the liquid from such pore completely and there is always some layer of liquid present on the passage walls, the effect of assumption of zero contact angle value and the presence of liquid layer may counteract each other to some degree. If the height of the liquid is small, let say below 1 cm, the correction ς·g·h is below 0.1% of atmospheric pressure and it is often neglected. The pore size determined by this equation is only an approximation of this actual passage size in the dry sample. The assumption of independent pores of different diameters is used but since pores can be interconnected in many samples, this simple transformation from pressure domain to pore size domain may have limited validity.

After the bubble point pressure and pore size was determined, the pV/T Master can be switched to Auto mode and various flow rates in increasing order can be applied for a certain amount of time resulting in corresponding pressure values to be obtained. Initial low flow rate result in establishing pressures just above the bubble point pressure and cause increase of number of spots emitting bubbles. At sufficiently high flows, the foaming effect is seen as the number of bubbles emitted from additional spots and intensity of bubbles from the same spots increases substantially. Further increase of flow rates does not seem to serve any useful purpose as many filter materials will not withstand such high pressure differential and their internal structure can be affected. Actually, for filters, only the largest pore sizes are of relevance as there is negligible flow fraction through the smallest ones.

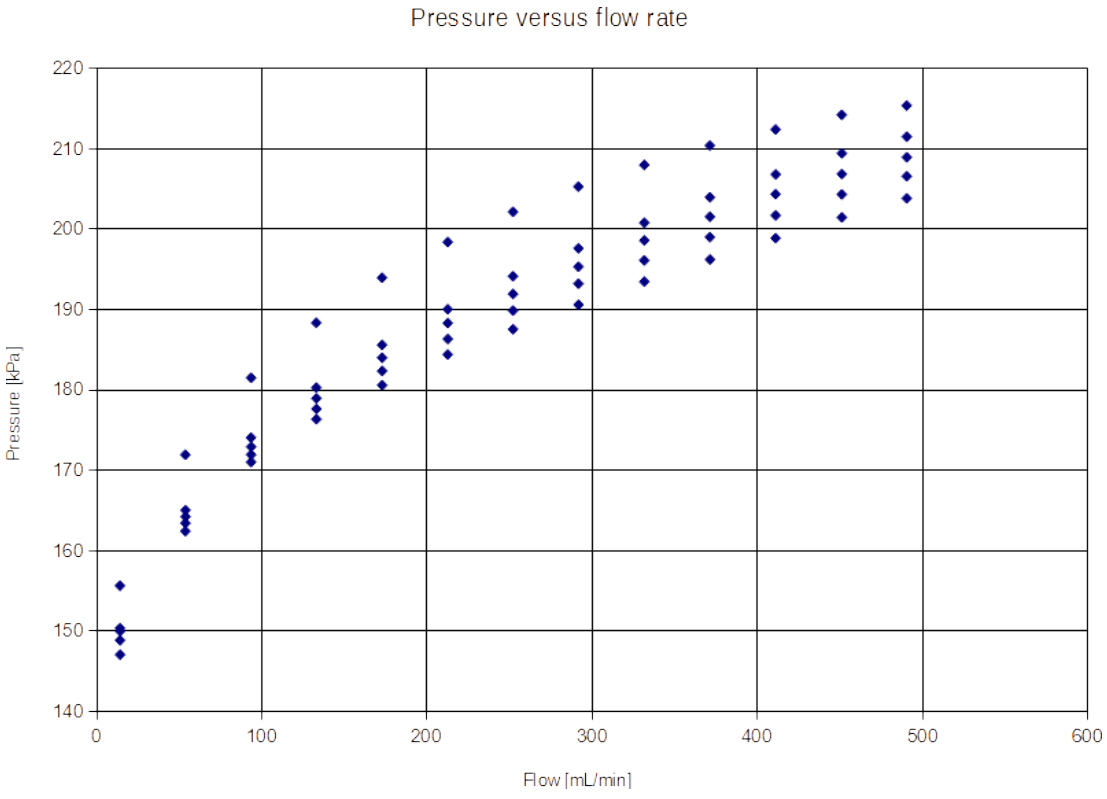

Wet run, five repetitions (Fig. 4)

The above chart shows five consecutive wet runs of the same sample using water as the wetting agent. The top series indicates the first run and subsequent runs fall below it. The sample was only wetted before the first run and about 10 mm of water was added on top of the wetted sample. Clearly the pressure values are shifted towards the lower values in each repetition. Inability to restore the same wetting conditions after cessation of flow, drying of the bottom of the specimen, occlusion of tiny air bubbles in the complex passages structure and possibly changes in the passages structure itself, are some of the reasons to be considered. The lesson is that in order to test repeatability, a new sample needs to be wetted each time the same way and fresh liquid needs to be used to reduce the number of factors affecting results.

However, another factor often overlooked in the CFP method is the time selection for establishing the steady-state pressure value for each flow. Some samples may require several minutes for reaching stable pressures and the long time is indicative of sample structure modification under the flow-pressure conditions. If there is no liquid above the sample, prolonged gas flow can dry up the sample. Depending on the flow rate used in drying, subsequent wetting and carrying out wet runs can cause pressures to fall below the dry runs. Therefore, the history of the sample is important. Also, this method, combined with temperature control and chemicals can be used for producing samples of desired properties.

The testing of CFP instruments and/or repeatability results are often reported based on usage of etched membranes. However, such membranes do not represent the actual structure complexity of filtering materials and therefore such specifications are of little value and create wrong expectations as to the behavior of real samples.

Let assume that in the dry run, M number of flow steps was carried out and the corresponding pressures were recorded after a steady state was achieved in each step. The flow and pressure values for the dry run can be denoted as (F_{di}, P_{di}), where index i runs from 1 to M. The same number of steps is usually used when the wet run is carried out. The flow and pressure values for wet run can be denoted as (F_{wi}, P_{wi}), where index i runs from 1 to M. Additionally, let the pressure value at bubble point be denoted as P_0. The flow steps are usually the same for both runs as the MFC can provide good repeatability of flow rates. Otherwise it is relatively easy to fit a curve into one of the data set and correct the pressure values corresponding to same flow values. The pore diameter or radius for each step can be determined using the eq. 3 or its simplified version. So, we have the following set of data:

Dry flow values:		$F_{d1}, F_{d2}, \dots, F_{dM}$	
Dry pressure values:		$P_{d1}, P_{d2}, \dots, P_{dM}$	
Wet flow values:		$F_{w1}, F_{w2}, \dots, F_{wM}$	
Wet pressure values:	P_0,	$P_{w1}, P_{w2}, \dots, P_{wM}$	
Pore size radii:	R_0,	$R_1, R_2, \dots, R_M$	(calculated using Eq. 5)

A different approach is proposed to provide pore size distribution from the experimental data. In the wet runs the flow consists of flow through capillaries and the diffusional flow, which is proportional to the pressure differential and sample area (Eq. 6). In the first wet step the flow value is the result of flows through pores from R_0 to R_1. Depending on the complexity of numerical treatment, one can calculate intermediate flows and pressures within the radii intervals. For simplicity and illustration of

the method, the first wet step can be approximated as the flow through N_{w1} capillaries (pores), each of radius R_1, and the contribution from the diffusional flow.

$$F_{w1} = \frac{\pi \cdot (P_{w1}^2 - P_a^2)}{16 \cdot \mu \cdot h \cdot P_a} \cdot A \cdot N_{w1} \cdot R_1^4 + \alpha \cdot (P_{w1} - P_a) \cdot A \qquad \text{(Eq. 6)}$$

Assuming that the proportionality constant α of the diffusional flow is known, as well as the effective surface area of the sample, the number N_{w1} can be calculated.

The next step flow F_{w2} can be presented as a sum of the flows through N_{w1} pores of R_1 radius but at P_{w2} value and the flow through a number of pores opened after pressure Pw1 with assumed pore size R_2.

$$F_{w2} = \frac{\pi \cdot (P_{w2}^2 - P_a^2)}{16 \cdot \mu \cdot h \cdot P_a} \cdot A \cdot N_{w1} \cdot R_1^4 + \frac{\pi \cdot (P_{w2}^2 - P_a^2)}{16 \cdot \mu \cdot h \cdot P_a} \cdot A \cdot N_{w2} \cdot R_2^4 + \alpha \cdot (P_{w2} - P_a) \cdot A \qquad \text{(Eq. 7)}$$

Assuming that the sum of the first and third part of the Eq. 7 is smaller then F_{w2}, then it is possible to calculate the N_{w2} number. Following the above assumptions for the first two steps, the more general equation can be presented for each J step.

$$F_{wJ} = \frac{\pi \cdot (P_{wJ}^2 - P_a^2)}{16 \cdot \mu \cdot h \cdot P_a} \cdot A \cdot \sum_{i=1}^{J} N_{wi} \cdot R_i^4 + \alpha \cdot (P_{wJ} - P_a) \cdot A \qquad \text{(Eq. 8)}$$

While this procedure can be improved by a more appropriate grouping of pore sizes, it provides in one form or another an iterative method of finding number of pores in a given pressure interval, assuming the last term of the sum is positive. If the last term in the sum in a given pressure interval is zero, then there are no new pores opened. If the last term starting since a certain pressure interval is negative, then the dynamic flow conditions, change of sample structural properties, or any other cause, may not allow further determination of any additional pore openings. Basically, the flow through the already opened pores becomes higher then predicted by the flow equation. Pores enlargements due to stretching of sample, more effective removal of wetting liquid from the passage channels, interconnected pores, and perhaps other factors need to be considered. In real samples the presumption that pores are emptied in decreasing order can be invalid as larger pores can be formed unexpectedly.

The numbers of capillaries calculated from the flow-pressures data can be presented either in a tabular form or graphed vs pressure or flow. Calculating the surface area of the capillaries in a given interval and summing them up yields the total area of flow through the sample per unit of area. Such parameter is indicative of effectiveness of a filter. For filters of a given porosity, the pressure increases after initial few steps are relatively small and the time of reaching a steady-state process is short. For samples that were not designed for filtering and have compact structure, like cotton-linen currency paper, the pressure increases tend to get higher, and smaller sizes pores are continually being opened and its structure being modified. Time of reaching a stable pressure takes much longer.